

## Article

# Model Discrimination for Hydrogen Peroxide Consumption towards $\gamma$ -Alumina in Homogeneous Liquid and Heterogeneous Liquid-Liquid Systems

Daniele Di Menno Di Bucchianico<sup>1,2</sup>, Wander Y. Perez-Sena<sup>1,3</sup>, Valeria Casson Moreno<sup>2</sup>, Tapio Salmi<sup>3</sup> and Sébastien Leveneur<sup>1,\*</sup> 

- <sup>1</sup> Normandie University, INSA Rouen, UNIROUEN, LSPC, EA4704 Rouen, France; daniele.di\_menno\_di\_bucchianico@insa-rouen.fr (D.D.M.D.B.); wander.perez\_sena@insa-rouen.fr (W.Y.P.-S.)
- <sup>2</sup> Dipartimento di Ingegneria Chimica, Civile, Ambientale e dei Materiali, Alma Mater Studiorum—Università di Bologna, via Terracini 28, 40131 Bologna, Italy; valeria.cassonmoreno@unibo.it
- <sup>3</sup> Laboratory of Industrial Chemistry & Reaction Engineering, Department of Chemical Engineering, Johan Gadolin Process Chemistry Centre, Åbo Akademi University, FI-20500 Åbo-Turku, Finland; tapio.salmi@abo.fi
- \* Correspondence: sebastien.leveneur@insa-rouen.fr

**Abstract:** The use of hydrogen peroxide as an oxidizing agent becomes increasingly important in chemistry. The example of vegetable oil epoxidation is an excellent illustration of the potential of such an agent. This reaction is traditionally performed by Prileschajew oxidation, i.e., by the in situ production of percarboxylic acids. Drawbacks of this approach are side reactions of ring-opening and thermal runaway reactions due to percarboxylic acid instability. One way to overcome this issue is the direct epoxidation by hydrogen peroxide by using  $\gamma$ -alumina. However, the reaction mechanism is not elucidated: does hydrogen peroxide decompose with alumina or oxidize the hydroxyl groups at the surface? The kinetics of hydrogen peroxide consumption with alumina in homogeneous liquid and heterogeneous liquid-liquid systems was investigated to reply to this question. Bayesian inference was used to determine the most probable models. The results obtained led us to conclude that the oxidation mechanism is the most credible for the heterogeneous liquid-liquid system.

**Keywords:** Bayesian statistics; kinetic modeling; model discrimination



**Citation:** Di Menno Di Bucchianico, D.; Perez-Sena, W.Y.; Casson Moreno, V.; Salmi, T.; Leveneur, S. Model Discrimination for Hydrogen Peroxide Consumption towards  $\gamma$ -Alumina in Homogeneous Liquid and Heterogeneous Liquid-Liquid Systems. *Processes* **2021**, *9*, 1476. <https://doi.org/10.3390/pr9081476>

Academic Editor: Chiing-Chang Chen

Received: 5 July 2021  
Accepted: 18 August 2021  
Published: 23 August 2021

**Publisher's Note:** MDPI stays neutral with regard to jurisdictional claims in published maps and institutional affiliations.



**Copyright:** © 2021 by the authors. Licensee MDPI, Basel, Switzerland. This article is an open access article distributed under the terms and conditions of the Creative Commons Attribution (CC BY) license (<https://creativecommons.org/licenses/by/4.0/>).

## 1. Introduction

As stated by Noyori et al. [1], hydrogen peroxide should be used instead of oxygen for oxygenation steps. One can cite the use of hydrogen peroxide for the epoxidation of olefin compounds.

In the market, the direct epoxidation by hydrogen peroxide as an oxidant offers advantages compared to the traditional processes, such as the chlorine-using non-catalytic process, co-epoxidation process, and catalytic processes based on organic peroxides and peracids (Figure 1). These traditional processes are characterized by producing large amounts of waste products, chloride-laden sewage, and acid wastes and present difficulty in separating the homogeneous catalysts. These processes are also capital-intensive [2].

Conversely, the epoxidation with hydrogen peroxide avoids producing toxic wastes, producing only water as a by-product, and using heterogeneous catalysts makes the separation step easier [4].

A broad range of solids has been tested as potential heterogeneous catalysts for the liquid phase epoxidation of olefins with hydrogen peroxide; catalysts such as framework-substituted molecular sieves, inorganic oxides, and supported catalysts, porous material encapsulated metal complexes, layered-type materials, peroxometalates, and supported porphyrin catalysts [2]. By testing systems based on different metals, titanium-based

catalysts are the most efficient heterogeneous catalysts for the epoxidation [5]; a well-known catalyst is the molecular sieve type Ti-Silicate-1 (TS-1) [6], which is capable of activating hydrogen peroxide and of epoxidizing different alkenes, but suffering from steric limitations, TS-1 is accessible only to small reactants and linear alkenes [7]. Different catalysts have been designed to overcome the steric limitations, such as Ti, Al-beta, and a zeolite with a three-dimensional pore structure [8].

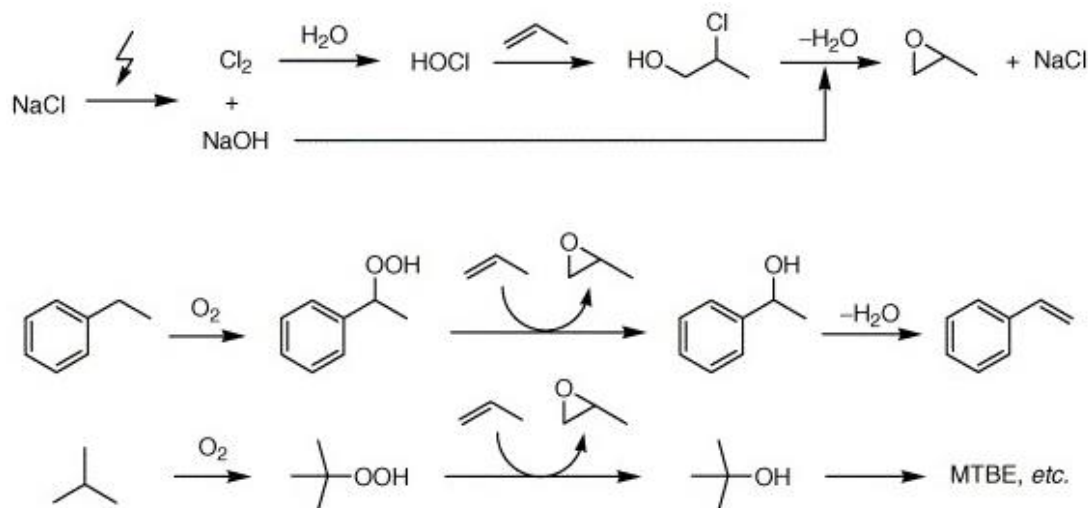


Figure 1. Mechanisms of traditional epoxidation process of olefins [3]. MTBE: Methyl tert-butyl ether.

In addition to the already tested transition metals, such as Ti, V, Cr, Mo, W, etc., a promising heterogeneous catalyst in epoxidation is alumina [4]. Alumina has proven to have an interesting catalytic activity in the epoxidation of several alkenes, from unreactive terminal-group alkenes to the highly reactive terpenes, using hydrogen peroxide, especially under nearly anhydrous conditions [4]. The nucleophilic character of its double bonds, the surface hydrophilicity, and the amount of weak Brønsted acid sites are remarkable factors for the high catalytic selectivity and activity of alumina [4].

The reaction mechanism of the  $Al_2O_3/H_2O_2$  catalyzed alkene epoxidation probably involves Al-OOH species (Figure 2) [4]. First, the alumina reacts with hydrogen peroxide, releasing water and producing the active species Al-OOH, which reacts with the olefins with the oxygen transferred to produce the resulting peroxide and the desired epoxide [4]. The catalytic activity of alumina is higher under anhydrous conditions because of the deactivation effect attributed to water and the adsorption of organic molecules on the catalyst surface. Conversely, water is fundamental in prolonging catalyst lifetime by shifting the equilibriums of the adsorption of by-products and preventing epoxide and hydrogen peroxide decomposition [5].

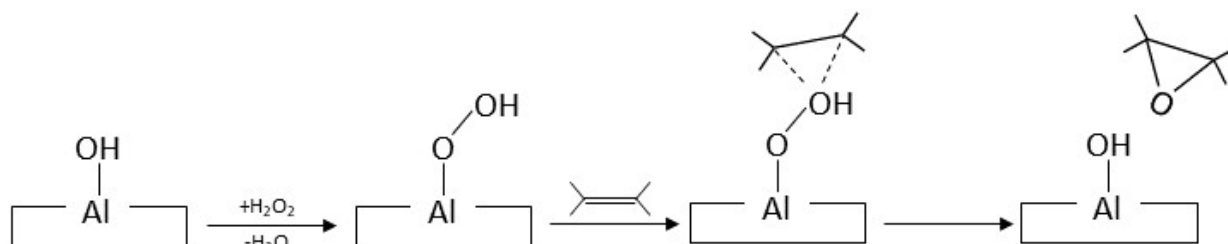


Figure 2. Mechanism of olefins epoxidation by alumina in the presence of hydrogen peroxide [4].

The use of alumina as a heterogeneous catalyst offers several advantages with respect to other systems with active metals. It is readily commercially available and has a relatively low cost, not only for the commercial chromatographic neutral alumina but also for other forms, such as the  $\gamma$ - $Al_2O_3$  that showed higher epoxidation activity compared to the first [2,6]. Furthermore, alumina can be recycled without the need for reactivation [7], and it does not show the problem of metal lixiviation due to solvent [6]. In particular, solvents as ethyl acetate increase the catalytic activity of alumina in epoxidation reactions [4]. The epoxidation reaction of vegetable oils or olefins by hydrogen peroxide can be homogeneously or heterogeneously catalyzed, but it requires an organic solvent in the reaction medium. The organic solvent is required to provide an efficient solubility of compounds, as vegetable oils are insoluble in the aqueous phase and improve the reaction and recovery of the epoxy product and catalyst [8,9]. Many parameters are considered in the choice of organic solvent from the process productivity point of view to the economic and safety points of view. In this field, ethyl acetate is commonly used since it is readily available, cheap, environmentally friendly, non-toxic to health, and forms a favorable azeotrope with water and hydrogen peroxide [4,9]. It has a medium polarity that leads to solubilization and extract polar and non-polar compounds. Several studies suggest that ethyl acetate solvent provides high epoxy conversions and leads to more straightforward product recovery and the homogeneous or heterogeneous catalyst [6,10].

Hence, the use of  $Al_2O_3$  in the presence of ethyl acetate as a solvent is a promising heterogeneous catalyzed way for the epoxidation with  $H_2O_2$  of olefins and more complex organic molecules, such as those derived from vegetable oils, which are becoming more used because of their availability from renewable resources [11], and it should be studied in more detail [12,13].

There are no studies on the kinetic modeling for this reaction system, to the best of our knowledge. It is not verified whether hydrogen peroxide oxidizes the Al-OH group or undergoes decomposition in the presence of  $\gamma$ -alumina. Therefore, the present research aims to develop kinetic models and verifies which reaction mechanism is the most probable via Bayesian inference [14].

## 2. Materials and Methods

The following chemicals were used: hydrogen peroxide 33% *w/w* stabilized, TECHNICAL, supplied by VWR Chemicals®; Ethyl Acetate, HiPerSolv CHROMANORM® for HPLC, supplied by VWR Chemicals® and  $\gamma$ -alumina, VERSAL™ Alumina GH, supplied by LaRoche Chemicals. For the analytical part, the following reagents were used: sulfuric acid, 96% for analysis ISO, supplied by PanReac AppliChem ITW Reagents; ammonium cerium (IV) sulfate solution 0.1 M, supplied by Honeywell Fluka™ and ferroin solution indicator (1,10-phenanthroline iron (II)-sulfate), AVS TITRINORM®, supplied by VWR Chemicals®.

The concentration of hydrogen peroxide (HP) was created by Ceric Sulfate Titration [13].

All experiments were performed in a 500 mL jacketed glass reactor, operating in batch mode, at atmospheric pressure (isobaric) and isothermal conditions. To avoid gas accumulation, a reflux condenser was placed on top of the reactor. At first, hydrogen peroxide solution was introduced into the reactor, and when the desired temperature was reached,  $\gamma$ -alumina was added, which was the time zero. Samples were withdrawn and analyzed during the reaction course. Tables 1 and 2 show the experimental matrix for homogeneous liquid and heterogeneous liquid-liquid systems.

**Table 1.** Experimental matrix for homogeneous liquid phase system. HP: hydrogen peroxide; W: water; 0: initial conditions.

Experiment	Temperature K	Catalyst Amount kg	HP Amount kg	HP0 mol/m <sup>3</sup>	W0 mol/m <sup>3</sup>
1	343.15	0.01012	0.2528	11,750	40,242
2	343.15	0.0152	0.2522	11,707	40,299
3	343.15	0.0203	0.2521	11,694	40,315
4	353.15	0.0021	0.2525	11,607	40,429
5	353.15	0.0052	0.2523	11,479	40,596
6	353.15	0.0102	0.2523	11,786	40,196
7	353.15	0.0152	0.252	11,683	40,330
8	353.15	0.0202	0.252	11,534	40,524
9	358.15	0.0102	0.2523	11,782	40,201

**Table 2.** Experimental matrix for heterogeneous liquid phase system. HP: hydrogen peroxide; W: water; 0: initial conditions; aq: aqueous phase; org: organic phase.

Experiment	Temperature K	Catalyst Amount kg	m <sub>aq,0</sub> kg	m <sub>org,0</sub> kg	[HP] <sub>aq,0</sub> mol/m <sup>3</sup>	[HP] <sub>org,0</sub> mol/m <sup>3</sup>	[W] <sub>aq,0</sub> mol/m <sup>3</sup>	[W] <sub>org,0</sub> mol/m <sup>3</sup>
1	324.05	0.00452	0.11297	0.11297	9622	911	42,979	1162
2	334.05	0.00452	0.11297	0.11297	9737	922	42,829	1158
3	343.95	0.00452	0.11297	0.11297	9531	903	43,097	1165
4	343.89	0.00678	0.11297	0.11297	10,039	951	42,437	1147
5	343.95	0.00904	0.11297	0.11297	9843	932	42,691	1154
6	334.139	0.00291	0.07281	0.14561	8802	888	44,047	1190
7	343.25	0.00291	0.07281	0.14561	8286	836	44,718	1209
8	343.47	0.00437	0.07281	0.14561	8830	891	44,011	1189
9	343.17	0.00582	0.07281	0.14561	8596	867	44,315	1198
10	333.15	0.00624	0.15601	0.07800	10,058	1740	42,411	1146
11	343.15	0.00624	0.15601	0.07800	10,427	1804	41,930	1133
12	343.15	0.00936	0.15601	0.07800	10,132	1753	42,437	1147
13	343.15	0.01248	0.15601	0.07800	10,301	1782	42,095	1138

### 3. Results and Discussion

Two different chemical systems were studied: a homogeneous liquid system with only a hydrogen peroxide solution and a heterogeneous liquid-liquid system in the presence of an aqueous hydrogen peroxide solution and ethyl acetate.

For both systems, in the absence of  $\gamma$ -alumina, there was no thermal decomposition of hydrogen peroxide in the temperature range 60–90 °C [15]. Thus, the thermal decomposition of hydrogen peroxide was not considered in the kinetic models. The distribution of hydrogen peroxide in the aqueous and organic phase was studied in the absence of  $\gamma$ -alumina.

The kinetic modeling follows different stages:

- Kinetic study of hydrogen peroxide decomposition or oxidation in the homogeneous liquid system;
- Evaluation of hydrogen peroxide distribution in the heterogeneous liquid-liquid;
- Kinetic study of hydrogen peroxide decomposition or oxidation in the heterogeneous liquid-liquid system.

### 3.1. Equilibrium Ratio

The equilibrium ratio for hydrogen peroxide can be defined as  $K_{HP} \approx \left( \frac{[HP]_{aq}}{[HP]_{org}} \right)_{equil.}$ , and its value can be affected by the weight percentage ratio of the organic-aqueous phase and temperature.

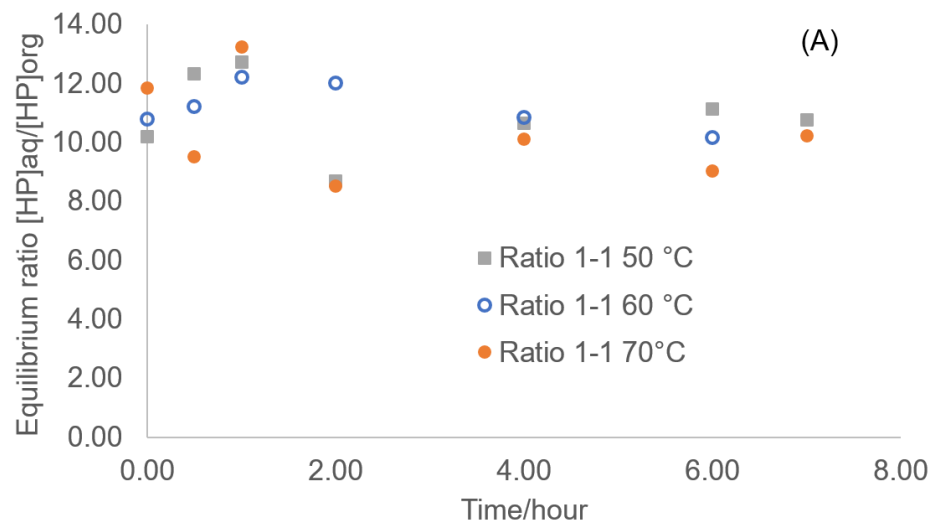
Three different ratios were tested as displayed in Table 3.

Figure 3 shows that the equilibrium is not sensitive to temperatures but to the ratio aqueous/organic. From these equilibrium experiments, values of  $K_{HP}$  can be calculated as displayed in the last column of Table 3.

For the water equilibrium ratio, the water solubility in ethyl acetate was used. From Klöker et al. [16], water solubility in ethyl acetate at 25 °C is 1.5 mol/L, so  $K_W$  is 37.

**Table 3.** Liquid-liquid ratio and calculated values of  $K_{HP}$ .

	wt% (HP Solution)	wt% (ethyl Acetate)	$K_{HP}$
Ratio 1-1	50.00	50.00	10.56
Ratio 1-2	33.33	66.67	9.91
Ratio 2-1	66.67	33.33	5.78



**Figure 3.** Cont.

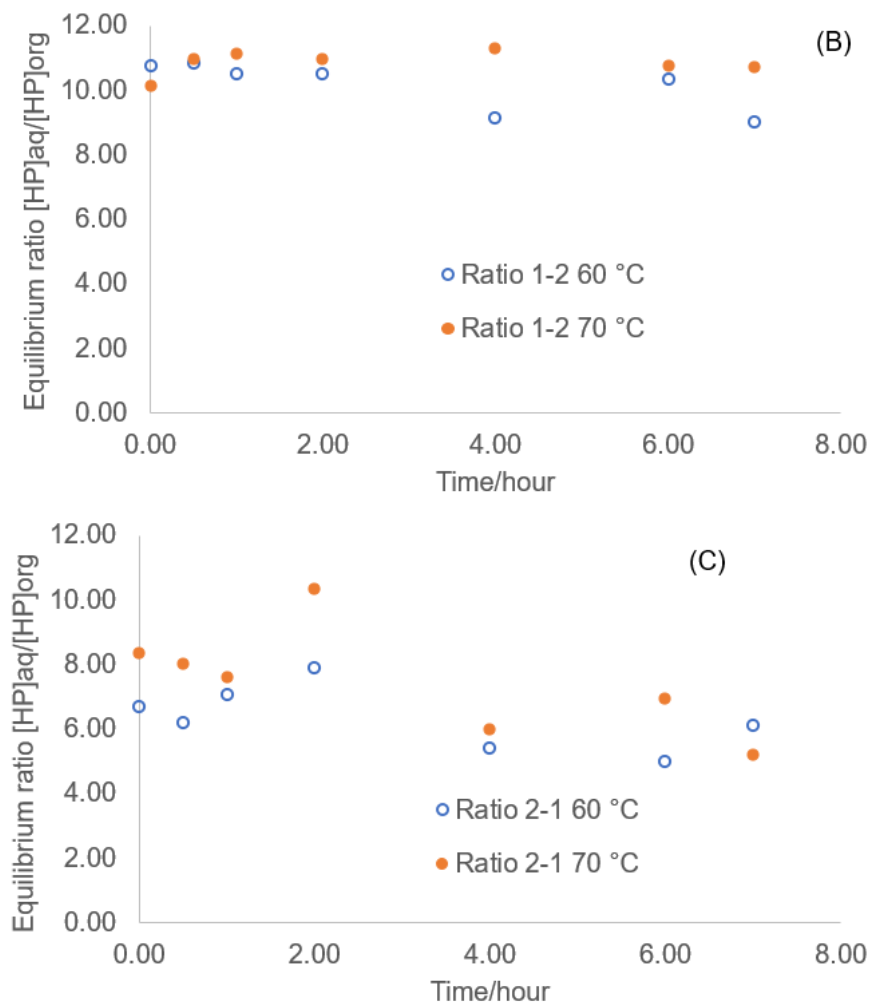


**Figure 3.** Evolution of the equilibrium ratio for hydrogen peroxide at different temperatures: (A) ratio 1-1; (B): ratio 1-2; (C): ratio 2-1.

### 3.2. Kinetic Models

Two reaction mechanisms were analyzed for both the homogeneous liquid phase and the heterogeneous liquid-liquid systems as described in the following sections.

#### 3.2.1. Kinetic Models for the Homogeneous Liquid Phase System

Two possible reaction mechanisms were studied: hydrogen peroxide decomposition by alumina and oxidation of Al-OH by hydrogen peroxide.

Model a: hydrogen peroxide decomposition by alumina

Figure 4 shows the assumed decomposition mechanism.



**Figure 4.** Reaction mechanism of hydrogen peroxide decomposition via HP adsorption.

The term \* is the active site. Quasi-steady state was applied to Step (1a), thus,

$$K_1 = K_{HP,ads} = \frac{H_2O_2^*}{[H_2O_2] \cdot *} \quad (1)$$

where  $H_2O_2^*$  is the adsorbed hydrogen peroxide species on  $\gamma$ -alumina.

Step (2a) is assumed to be the rate-determining step.

$$R_{Decomp,Hom} = R_2 = k_2 \cdot H_2O_2^* \cdot \omega_{cat} \quad (2)$$

where  $\omega_{cat}$  is the catalyst loading in kg/L.

Balance on active sites leads to

$$* + H_2O_2^* = 1 \quad (3)$$

Hence,

$$K_1 = \frac{1 - *}{[H_2O_2] \cdot *} \iff * = \frac{1}{(K_{HP,ads} \cdot [H_2O_2] + 1)} \quad (4)$$

Thus, the rate of HP decomposition over  $\gamma$ -alumina can be expressed as

$$R_{Decomp,Hom} = k_{Decomp,Hom} \cdot K_{HP,ads} \cdot [H_2O_2] \cdot \frac{1}{(K_{HP,ads} \cdot [H_2O_2] + 1)} \cdot \omega_{cat} \quad (5)$$

Model b: oxidation of hydroxyl group (Al-OH) by hydrogen peroxide

Figure 5 shows the reaction mechanism based on the work of Mandelli et al. [4].

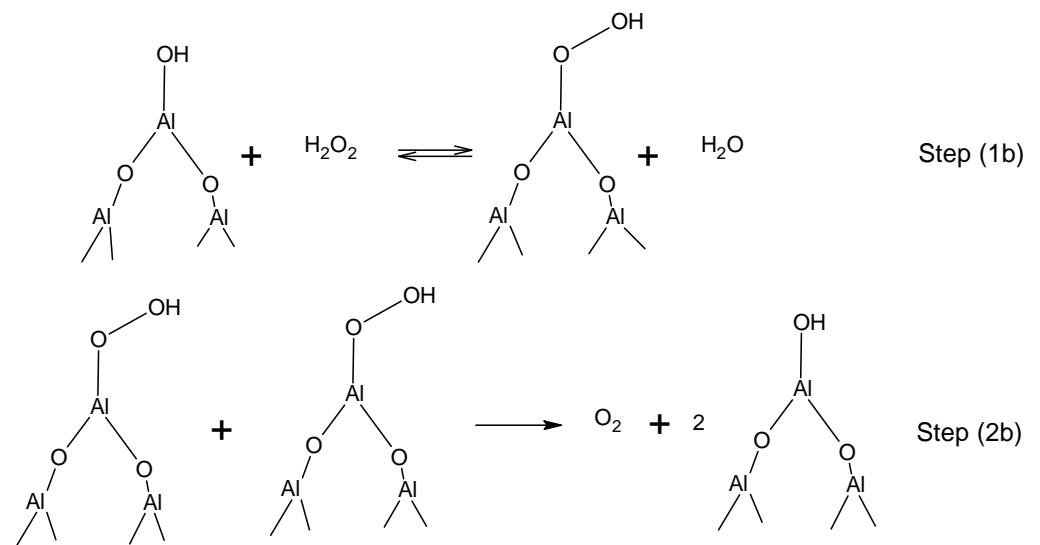


Figure 5. Simplified mechanism of oxidation.

Step (1b) is assumed to be reversible and faster than Step (2b), thus,

$$K_1 = \frac{\theta_{AlOOH} \cdot [H_2O]}{\theta_{AlOH} \cdot [H_2O_2]} \quad (6)$$

The rate-determining step is Step (2b)

$$R_{Oxidation,Hom,Model2} = R_2 = k_2 \cdot \theta_{AlOOH}^2 \cdot \omega_{cat} \quad (7)$$

Balance on hydroxyl sites leads to

$$\theta_{AlOH} + \theta_{AlOOH} = 1 \iff \theta_{AlOOH} = 1 - \theta_{AlOH} \quad (8)$$

By combining (7) and (8), the equilibrium constant of step (1b) can be expressed as

$$K_1 = \frac{(1 - \theta_{AlOH}) \cdot [H_2O]}{\theta_{AlOH} \cdot [H_2O_2]} \iff \theta_{AlOH} = \frac{[H_2O]}{K_1 \cdot [H_2O_2] + [H_2O]} \quad (9)$$

Rate of hydroxyl oxidation by HP over  $\gamma$ -alumina can be expressed as

$$R_{Oxidation,Hom} = k_{Oxidation,Hom} \cdot \left( \frac{K_1 \cdot [H_2O_2]}{(K_1 \cdot [H_2O_2] + [H_2O])} \right)^2 \cdot \omega_{cat} \quad (10)$$

### 3.2.2. Kinetic Models for the Heterogeneous Liquid-Liquid System

Model c: decomposition of hydrogen peroxide

Figure 6 shows the reaction mechanism.

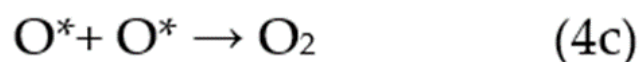
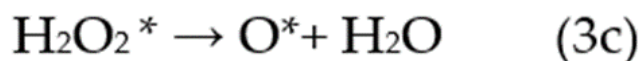
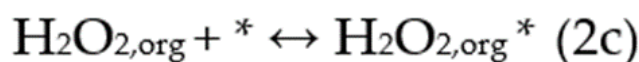
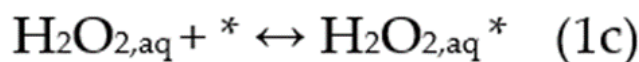


Figure 6. Decomposition of hydrogen peroxide in the heterogeneous liquid-liquid system.

A quasi-steady approach was applied to Steps (1c) and (2c); thus, the adsorption constant for HP from aqueous and organic phases can be expressed as

$$K_{HP,ads,aq} = \frac{H_2O_{2,aq}^*}{[H_2O_2]_{aq} \cdot *} \quad \text{and} \quad K_{HP,ads,org} = \frac{H_2O_{2,org}^*}{[H_2O_2]_{org} \cdot *} \quad (11)$$

Balance on sites leads to

$$* + H_2O_{2,aq}^* + H_2O_{2,org}^* = 1 \quad \text{equivalent to} \quad * = \frac{1}{1 + K_{HP,ads,aq} \times [H_2O_2]_{aq} + K_{HP,ads,org} \times [H_2O_2]_{org}} \quad (12)$$

Step (3c) is assumed to be the rate-determining step. Both species  $H_2O_{2,aq}^*$  and  $H_2O_{2,org}^*$  are supposed to be the same; thus, the rate of decomposition can be expressed as

$$\begin{aligned} R_{Decomp,Het} = R_3 &= k_3 \cdot ([H_2O_2]_{aq}^* + [H_2O_2]_{org}^*) \cdot \omega_{cat} \\ &= k_{Decomp0,Het} \cdot \left( \frac{K_{HP,ads,aq} \cdot [H_2O_2]_{aq} + K_{HP,ads,org} \cdot [H_2O_2]_{org}}{1 + K_{HP,ads,aq} \times [H_2O_2]_{aq} + K_{HP,ads,org} \times [H_2O_2]_{org}} \right) \cdot \omega_{cat} \end{aligned} \quad (13)$$

Model d: oxidation of hydroxyl by hydrogen peroxide

Figure 7 shows the reaction mechanism in the liquid-liquid reaction system.

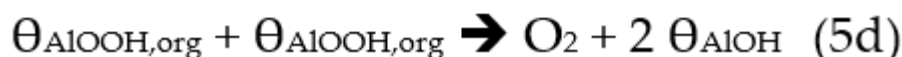
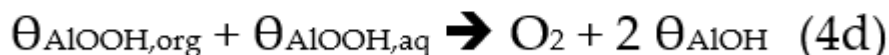
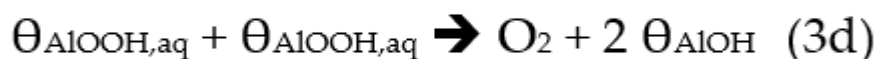


Figure 7. Oxidation mechanism.

Balance on hydroxyl sites leads to

$$\theta_{AlOOH,org} + \theta_{AlOOH,aq} + \theta_{AlOH} = 1 \quad (14)$$

Steps 1d and 2d are assumed to be fast and reversible; thus, the equilibrium constants can be expressed as

$$K_{1,aq} = \frac{\theta_{AlOOH,aq} \cdot [H_2O]_{aq}}{\theta_{AlOH} \cdot [H_2O_2]_{aq}} \quad \text{and} \quad K_{1,org} = \frac{\theta_{AlOOH,org} \cdot [H_2O]_{org}}{\theta_{AlOH} \cdot [H_2O_2]_{org}} \quad (15)$$

Steps (3d)–(5d) are the rate-determining steps; thus, the rate of oxidation in the heterogeneous liquid-liquid system can be derived as

$$R_{Oxidation,Het} = R_3 + R_4 + R_5 \quad (16)$$

Rate constants for  $R_3$ ,  $R_4$  and  $R_5$  can be considered to be similar.

$$\begin{aligned} R_{Oxidation,Het} &= k_{Oxidation,Het} \cdot \left( \theta_{AlOOH,aq}^2 + \theta_{AlOOH,org}^2 + \theta_{AlOOH,aq} \cdot \theta_{AlOOH,org} \right) \cdot \omega_{cat} \\ &= k_{Oxidation,Het} \cdot \left( \left( \frac{K_{1,aq} \cdot [H_2O_2]_{aq}}{[H_2O]_{aq}} \right)^2 + \left( \frac{K_{1,org} \cdot [H_2O_2]_{org}}{[H_2O]_{org}} \right)^2 + \left( \frac{K_{1,aq} \cdot [H_2O_2]_{aq}}{[H_2O]_{aq}} \right) \right. \\ &\quad \left. \cdot \left( \frac{K_{1,org} \cdot [H_2O_2]_{org}}{[H_2O]_{org}} \right) \right) \cdot \left( \frac{1}{\frac{K_{1,aq} \cdot [H_2O_2]_{aq}}{[H_2O]_{aq}} + \frac{K_{1,org} \cdot [H_2O_2]_{org}}{[H_2O]_{org}} + 1} \right)^2 \cdot \omega_{cat} \end{aligned} \quad (17)$$

### 3.3. Material Balances

The molar balances are defined considering the reaction system as an isothermal and isobaric batch and accounting for hydrogen peroxide and water as principal compounds. The production of oxygen was not considered in the material balances.

#### 3.3.1. Homogeneous Liquid Phase System

In this case, the molar balance of the compound ( $i$ ) is written as:

$$\frac{dC_i}{dt} = v_{i,j} R_j \quad (18)$$

where:

- $C_i$  concentration of compound ( $i$ ) (mol);
- $v_{i,j}$  is the stoichiometric coefficient of the compound ( $i$ ) in the reaction ( $j$ );
- $R_j$  is the rate of the reaction ( $j$ ) (mol/(m<sup>3</sup> s)).

For Model a, the material balances on hydrogen peroxide and water are

$$\frac{dC_{HP}}{dt} = -R_{Decomp,Hom} \quad (19)$$

$$\frac{dC_W}{dt} = R_{Decomp,Hom} \quad (20)$$

For Model b, material balances on hydrogen peroxide and water are

$$\frac{dC_{HP}}{dt} = -R_{Oxidation,Hom} \quad (21)$$

$$\frac{dC_W}{dt} = R_{Oxidation,Hom} \quad (22)$$

### 3.3.2. Heterogeneous Liquid-Liquid System

In this case, it is necessary to consider the balance for each compound in each phase, i.e., in the aqueous and organic phases. In the aqueous phase, the molar balance of compound ( $i$ ) is written as Equation (23):

$$\frac{dn_{i,aq}}{dt} = \sum v_{ij} V_{aq} R_{aq,j} - N_i A \quad (23)$$

where:

- $n_{i,aq}$  moles of compound ( $i$ ) in the aqueous phase (mol);
- $v_{ij}$  is the stoichiometric coefficient of the compound ( $i$ ) in the reaction ( $j$ );
- $V_{aq}$  is the aqueous phase volume ( $m^3$ );
- $R_{aq,j}$  is the rate of the reaction ( $j$ ) in the aqueous phase ( $mol/(m^3 s)$ );
- $N_i$  is the mass flux of the compound ( $i$ ) from the aqueous to the organic phase ( $mol/(s m^2)$ );
- $A$  is the interfacial surface between the two phases ( $m^2$ ).

Introducing the parameters:  $\alpha = \frac{V_{aq}}{V_R}$ ,  $a = \frac{A}{V_R}$ .

Considering the aqueous phase volume constant ( $V_{aq} = constant$ ) on time, Equation (23) becomes:

$$\frac{dC_{i,aq}}{dt} = \sum v_{ij} R_{aq,j} - \frac{N_i A}{V_{aq}} \quad (24)$$

where,  $C_{i,aq}$  is the concentration of compound ( $i$ ) in the aqueous phase ( $mol/m^3$ );

Then,

$$\frac{dC_{i,aq}}{dt} = \sum v_{ij} R_{aq,j} - \frac{N_i a}{\alpha} \quad (25)$$

In the organic phase, the molar balance of compound ( $i$ ) is written as:

$$\frac{dn_{i,org}}{dt} = \sum v_{ij} V_{org} R_{org,j} + N_i A \quad (26)$$

where:

- $n_{i,org}$  moles of compound ( $i$ ) in the organic phase (mol);
- $v_{ij}$  is the stoichiometric coefficient of the compound ( $i$ ) in the reaction ( $j$ );
- $V_{org}$  is the organic phase volume ( $m^3$ );
- $R_{org,j}$  is the rate of the reaction ( $j$ ) in the organic phase ( $mol/(m^3 s)$ );
- $N_i$  is the mass flux of the compound ( $i$ ) from the aqueous to the organic phase ( $mol/(s m^2)$ );
- $A$  is the interfacial surface between the two phases ( $m^2$ ).

Introducing the parameter  $\beta = \frac{V_{org}}{V_R} = (1 - \alpha)$

Dividing by the organic phase volume, supposed to be constant during the reaction:

$$\frac{dC_{i,org}}{dt} = \sum v_{ij}R_{org,j} + \frac{N_i A}{V_{org}} \quad (27)$$

where  $C_{i,org}$  is the concentration of compound ( $i$ ) in the organic phase;

$$\frac{dC_{i,org}}{dt} = \sum v_{ij}R_{org,j} + \frac{N_i a}{(1 - \alpha)} \quad (28)$$

Then, multiplying (25) and (28) by  $\alpha$  and  $(1 - \alpha)$ , respectively:

$$\frac{dC_{i,aq}}{dt}\alpha = \sum v_{ij}R_{aq,j}\alpha - N_i a \quad (29)$$

$$\frac{dC_{i,org}}{dt}(1 - \alpha) = \sum v_{ij}R_{org,j}(1 - \alpha) + N_i a \quad (30)$$

By summing Equations (29) and (30), the result is

$$\frac{dC_{i,aq}}{dt}\alpha + \frac{dC_{i,org}}{dt}(1 - \alpha) = \sum v_{ij}R_{aq,j}\alpha + \sum v_{ij}R_{org,j}(1 - \alpha) \quad (31)$$

Assuming fast kinetics and thus rapid mass transfer [17], the equilibrium molar ratio can be approximated as:

$$K_i = \frac{[i_{aq}]^*}{[i_{org}]^*} \approx \left( \frac{[i_{aq}]}{[i_{org}]} \right)_{equil.} \quad (32)$$

Thus, material balances in the aqueous and organic phase become

$$\frac{dC_{i,aq}}{dt} = \frac{1}{\alpha + \frac{1-\alpha}{K_i}} (\sum v_{ij}R_{aq,j}\alpha + \sum v_{ij}R_{org,j}(1 - \alpha)) \quad (33)$$

$$\frac{dC_{i,org}}{dt} = \frac{1}{\alpha K_i + (1 - \alpha)} (\sum v_{ij}R_{aq,j}\alpha + \sum v_{ij}R_{org,j}(1 - \alpha)) \quad (34)$$

In this system, the decomposition or oxidation rates is the same in both phases:

$$R_{Decomp,aq} = R_{Decomp,org} = R_{Decomp} \text{ or } R_{Oxidation,aq} = R_{Oxidation,org} = R_{Oxidation}$$

The general molar balance obtained in each phase can be applied explicitly to hydrogen peroxide and water in aqueous and organic phases, respectively.

For Model c, the molar balance expressions for hydrogen peroxide in the decomposition reaction become:

$$\frac{dC_{HP,aq}}{dt} = \frac{1}{\alpha + \frac{1-\alpha}{K_{HP}}} (-R_{dec,aq}\alpha - R_{dec,org}(1 - \alpha)) = \frac{-1}{\alpha + \frac{1-\alpha}{K_{HP}}} R_{Decomp,Het} \quad (35)$$

$$\frac{dC_{HP,org}}{dt} = \frac{1}{\alpha K_{HP} + (1 - \alpha)} (-R_{dec,aq}\alpha - R_{dec,org}(1 - \alpha)) = \frac{-R_{Decomp,Het}}{\alpha K_{HP} + (1 - \alpha)} \quad (36)$$

While for the water, the expressions become:

$$\frac{dC_{W,aq}}{dt} = \frac{R_{Decomp,Het}}{\alpha + \frac{1-\alpha}{K_W}} \quad (37)$$

$$\frac{dC_{W,org}}{dt} = \frac{R_{Decomp,Het}}{\alpha K_W + (1 - \alpha)} \quad (38)$$

For Model d, the molar balance expressions for hydrogen peroxide in the decomposition reaction become:

$$\frac{dC_{HP,aq}}{dt} = \frac{-1}{\alpha + \frac{1-\alpha}{K_{HP}}} \cdot R_{Oxidation,Het} \quad (39)$$

$$\frac{dC_{HP,org}}{dt} = \frac{-R_{Oxidation,Het}}{\alpha K_{HP} + (1-\alpha)} \quad (40)$$

While for the water, the expressions become

$$\frac{dC_{W,aq}}{dt} = \frac{R_{Oxidation,Het}}{\alpha + \frac{1-\alpha}{K_W}} \quad (41)$$

$$\frac{dC_{W,org}}{dt} = \frac{R_{Oxidation,Het}}{\alpha K_W + (1-\alpha)} \quad (42)$$

The partition coefficients  $K_{HP}$  and  $K_W$  have been experimentally evaluated and then, used as fixed constant in the kinetic modeling.

### 3.4. Modeling

Athena Visual Studio was used to solve the Ordinary Differential EquationS (ODEs) and estimate the kinetic constants through Bayesian statistics [18,19]. For the regression stage, concentrations of hydrogen peroxide in the aqueous and organic phases were used.

The Differential-Algebraic solver DDAPLUS was used for Equations (19)–(22) and (35)–(42). GREGPLUS package was used for the parameter estimation stage. This package minimizes the objective function  $S(\theta)$  (Equation (43)), and calculates the maximum posterior probability density of the different estimated parameters  $\theta$  and the values of the posterior distribution of the tested models [18,19]:

$$S(\theta) = (n + m + 1) \cdot \ln|v(\theta)| \quad (43)$$

where,  $n$  is the number of events in response,  $m$  is the number of responses and  $|v(\theta)|$  is the determinant of the covariance matrix of the responses.

Each element of this matrix is defined as:

$$v_{ij}(\theta) = \sum_{u=1}^n [Y_{iu} - f_{iu}(\xi_u, \theta)] \cdot [Y_{ju} - f_{ju}(\xi_u, \theta)] \quad (44)$$

with  $Y_{iu}$  the experimental concentration and  $f_{iu}(\xi_u, \theta)$  the estimated value for the response  $i$  and event  $u$ ;  $Y_{ju}$  the experimental concentration and  $f_{ju}(\xi_u, \theta)$  the estimated value for response  $j$  and event  $u$ .

The precision of the estimated parameters was evaluated by the marginal Highest Posterior Density (HPD). The 95% HPD was calculated by the GREGPLUS package.

The parameters to be estimated are the adsorption constants, the rate constants, and the activation energies. The modified Arrhenius equation is used in order to decrease the correlation between the pre-exponential factor and the activation energy:

$$k_i(T_R) = k_i(T_{ref}) \cdot \exp\left(-\frac{E_{a_i}}{T_R} \left(\frac{1}{T_R} - \frac{1}{T_{ref}}\right)\right) \quad (45)$$

where,  $T_{ref}$  is the reference temperature ( $T_{ref} = 343.15$  K) chosen in the considered experimental temperature range.

To discriminate between both models, the probability  $M_\infty$ , describing the experimental concentrations  $Y$  within the error space  $Y$ , was calculated [18,19]. This probability,  $p(M_\infty|Y, Y)$ , also known as the posterior distribution is:

$$p(M_\infty|Y, Y) = \frac{L(Y, Y|M_\infty) \cdot p(M_\infty)}{C} \quad (46)$$

where  $L(Y, Y|M_\infty)$  is the likelihood function evaluating the probability of the experimental concentrations  $Y$  generated by the model  $M_\infty$  with its parameter vector  $\theta$ . The term  $C$  is a normalization constant. The probability  $p(M_\infty)$  is the prior distribution considering the experimentalist knowledge. The boundaries of the estimated parameters are known, and replicate experiments evaluate the error space.

The model discrimination was evaluated by the determination of the normalized posterior probabilities (Equation (47)).

$$\pi(M_\infty|Y, Y) = \frac{p(M_\infty|Y, Y) * 100}{\sum_k p(M_\infty|Y, Y)} \quad (47)$$

In the first stage, kinetic and adsorption constants from experiments in the homogeneous liquid phase were estimated. Then, these constants were estimated for the heterogeneous liquid-liquid system.

#### 3.4.1. Homogeneous Liquid Phase System

Models a and b were tested toward experiments in the homogeneous liquid phase (Table 1).

For Model a, Table 4 shows the values of the estimated kinetic constants with their credible intervals. The credible intervals, represented by the HPD values, are relatively low showing the adequate variation of the operating conditions. The strong correlation (shown in Table 5) between the rate constant  $k_{Decomp}$  (T = 343.15 K) and the adsorption constant  $K_{HP}$  is linked to the difficulty of estimating both constants efficiently.

Figure 8 displays the parity plot between the experimental and simulated concentrations of hydrogen peroxide. One can notice that Model a (Figure 8A) can predict the hydrogen peroxide concentration.

In Model b, the credible intervals for the estimated kinetic constants are lower than for Model a (as shown in Table 4). Nevertheless, there is still a strong correlation between the estimated rate constant and  $K_1$  (see Table 5). Figure 8B shows that also Model b can predict the concentration of hydrogen peroxide.

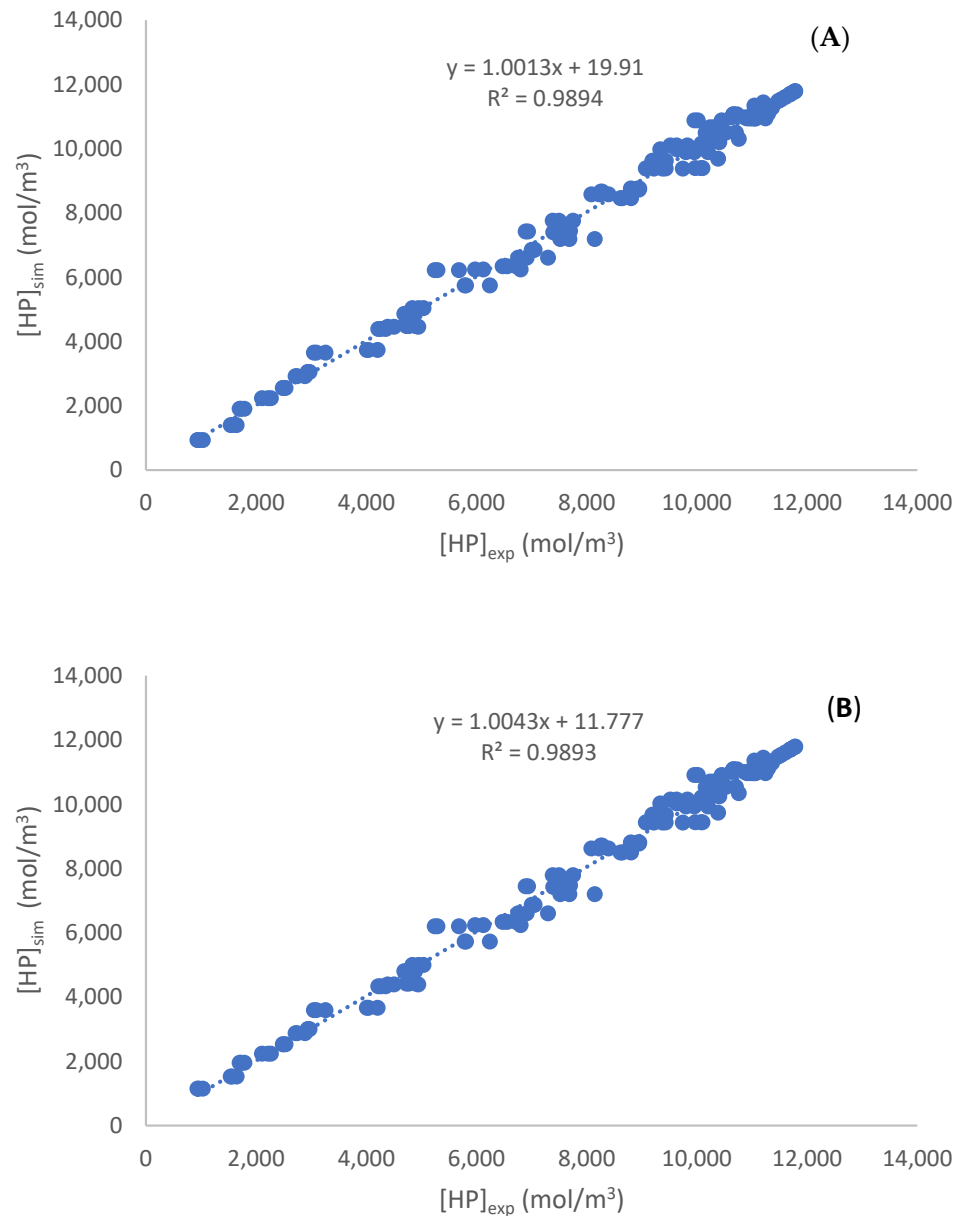
The posterior probability densities of both mechanisms are similar, as well as the parity plots (Figure 8). Hence, it is challenging to discriminate both models, even if HPD values for the Model b (oxidation) are lower than for the Model a (decomposition). The goal of this study is to ease the kinetic modeling for heterogeneous systems, in other words, to obtain reliable initial guess values.

**Table 4.** Estimated kinetic constants and credible intervals for Models a and b for the homogeneous liquid phase system.

Model a (Decomposition)				Model b (Oxidation)			
Kinetic Constants	Units	Estimate	HPD/%	Kinetic Constants	Units	Estimate	HPD/%
$k_{Decomp}$ (T = 343.15 K)	mol/kg/s	0.017	31.74	$k_{Oxid}$ (T = 343.15 K)	mol/kg/s	0.009	8.98
$Ea_{Decomp}$	J/mol	68,752.51	4.41	$Ea_{Oxid}$	J/mol	68,918.58	4.45
$K_{HP}$	m <sup>3</sup> /mol	$4.40 \times 10^{-5}$	42.45	$K_1$	-	15.05	15.43

**Table 5.** Normalized covariance matrix for the estimated kinetic constants for Models a and b for the homogeneous liquid phase system.

Model a				Model b			
Kinetic Constants	$k_{Decomp}$ (T = 343.15 K)	$Ea_{Decomp}$	$K_{HP}$	Kinetic Constants	$k_{Oxid}$ (T = 343.15 K)	$Ea_{Oxid}$	$K_1$
$k_{Decomp}$ (T = 343.15 K)	1			$k_{Oxid}$ (T = 343.15 K)	1		
$Ea_{Decomp}$	0.302	1		$Ea_{Oxid}$	0.357	1	
$K_{HP}$	−0.998	−0.28	1	$K_1$	−0.979	−0.274	1

**Figure 8.** Parity plot for the homogeneous liquid phase using Model a (A) and Model b (B).

### 3.4.2. Heterogeneous Liquid-Liquid Phase System

For the case of Model c (decomposition), the adsorption constant  $K_{HP,ads,aq}$  was fixed to  $4.40 \times 10^{-5} \text{ m}^3/\text{mol}$ , which is the value estimated in the homogeneous liquid phase. Table 6 shows the resulting kinetic constants and their credible intervals (HPD). The HPD is low for the kinetic constants but high for the adsorption constant. From Table 7, the correlation between the estimated parameters is low, except for the parameters between  $k_{Decomp}$

( $T = 343.15$  K) and  $K_{HP,ads,org}$ . Figure 9A shows the parity plot for hydrogen peroxide concentration in the aqueous and organic phases from which Model c can correctly predict both concentrations.

For Model d (oxidation), the equilibrium constant  $K_{1,aq}$  obtained from the homogeneous liquid system was used. Modeling revealed that the values for  $K_{1,org}$  tend to zero, indicating that this adsorption phenomenon can be neglected. Table 6 shows that the estimated kinetic constants are reliable due to the low value of HPD. Table 7 shows the low correlation between rate constant and activation energy. Figure 9B shows the parity plot for hydrogen peroxide concentration in the aqueous and organic phases from which Model d can correctly predict both concentrations.

The posterior probability density was found to be  $10^{89}$  for Model c, and  $10^{90}$  for Model d (Table 8). The estimation of these values allows calculating the posterior probability share for each Model. Table 8 also shows objective function values for each Model in the heterogeneous liquid phase system. The posterior probability share represents 90% for Model d compared to Model c, and the objective function value for Model d is lower than that for Model c, confirming that hydrogen peroxide oxidizes the hydroxyl group on alumina.

Due to space limitation, the residual plots (Figure A1) and fit of Model d to experimental data are shown in Supporting Information (Figure A2). Figure A1 shows that the residuals are normally distributed versus time, experimental, and estimated concentration of hydrogen peroxide obtained with Model d.

Figures A2–A5 show 95% prediction intervals for the concentration of hydrogen peroxide in the aqueous and organic phases, using the average of the experimental data and setting  $K_{1,org} = 0$  and  $K_{1,aq} = 15.05$  for Experiments 2, 3, 9 and 12. Model d fits the experimental data.

**Table 6.** Estimated kinetic constants and credible intervals for Models c and d for the heterogeneous liquid phase system.

Model c (Decomposition)				Model d (Oxidation)			
Kinetic Constants	Units	Estimate	HDP/%	Kinetic Constants	Units	Estimate	HDP/%
$k_{Decomp}$ ( $T = 343.15$ K)	mol/kg/s	0.007	13.69	$k_{Oxid}$ ( $T = 343.15$ K)	mol/kg/s	0.004	2.18
$Ea_{Decomp}$	J/mol	51,981.53	17.78	$Ea_{Oxid}$	J/mol	52,444.63	14.04
$K_{HP,ads,aq}$	$m^3/mol$	$4.40 \times 10^{-5}$		$K_{1,aq}$	-	15.05	
$K_{HP,ads,org}$	$m^3/mol$	$9.81 \times 10^{-5}$	90.84	$K_{1,org}$	-	~0	

**Table 7.** Normalized covariance matrix for the estimated kinetic constants for Models c and d for the heterogeneous liquid phase system.

Kinetic Constants	Model c (Decomposition)				Kinetic Constants	Model d (Oxidation)			
	$k_{Decomp}$ ( $T = 343.15$ K)	$Ea_{Decomp}$	$K_{HP,aq}$	$K_{HP,org}$		$k_{Oxid}$ ( $T = 343.15$ K)	$Ea_{Oxid}$	$K_{1,aq}$	$K_{1,org}$
$k_{Decomp}$ ( $T = 343.15$ K)	1				$k_{Oxid}$ ( $T = 343.15$ K)	1			
$Ea_{Decomp}$	0.07	1			$Ea_{Oxid}$	0.183	1		
$K_{HP,ads,aq}$	-	-	-		$K_{1,aq}$	-	-	-	
$K_{HP,ads,org}$	-0.974	-0.034	0	1	$K_{1,org}$	-	-	-	-

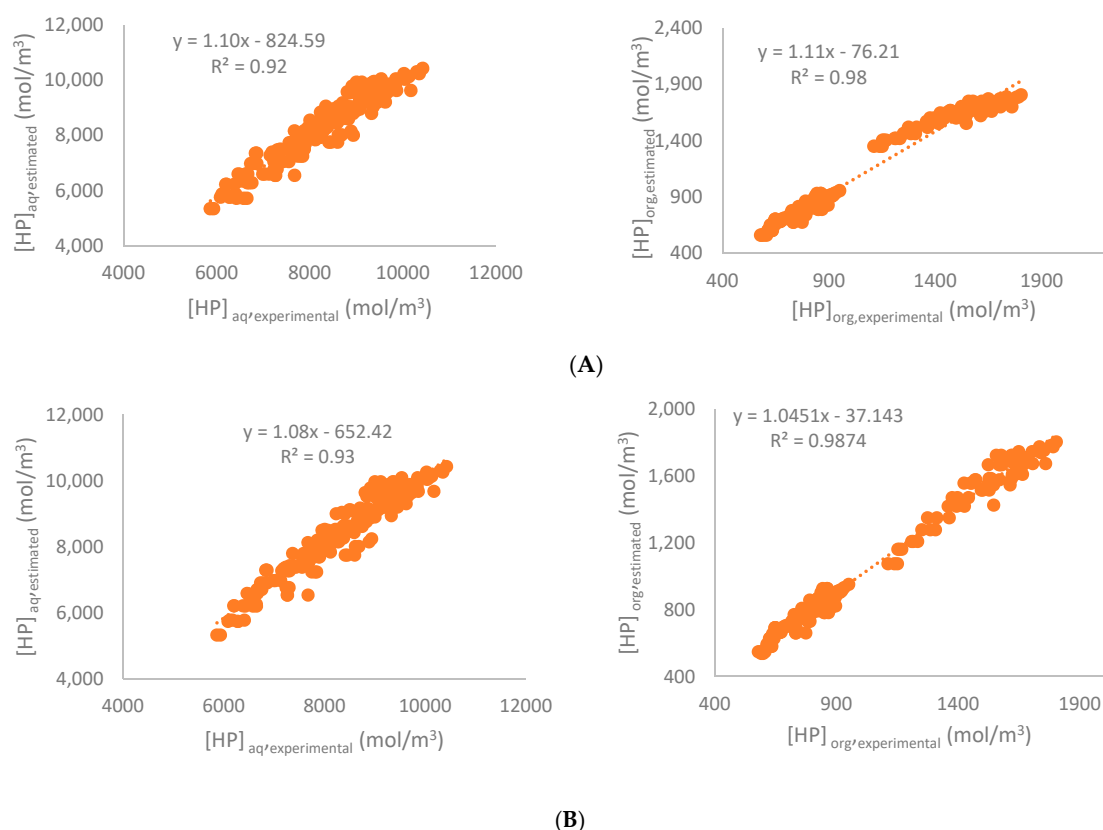


Figure 9. Parity plot for the heterogeneous liquid phase system using Model c (A) and Model d (B).

Table 8. Modeling results from Bayesian statistics for the case of heterogeneous liquid-liquid phase system.

Model	Objective Function $S(\theta)$	Posterior Probability $p(M_\infty   Y, \mathbf{Y})$	Posterior Probability Share % $\pi(M_\infty   Y, \mathbf{Y})$ in %
c	$7.77 \times 10^3$	$1.00 \times 10^{90}$	9.09
d	$7.46 \times 10^3$	$1.00 \times 10^{91}$	90.91

#### 4. Conclusions

Hydrogen peroxide becomes increasingly important as an oxidizing agent. However, there is a lack of knowledge concerning its reaction mechanism: does hydrogen peroxide decompose to produce oxygen leading to oxidation, or does hydrogen peroxide oxidize the catalyst surface? This manuscript studied this matter by investigating two reaction systems: hydrogen peroxide consumption with  $\gamma$ -alumina in the homogeneous liquid phase versus in the heterogeneous liquid-liquid system.

Experiments were performed in batch conditions in isothermal mode by varying operating conditions such as temperature as well as catalyst and chemicals amount. The distribution coefficient of hydrogen peroxide between the organic and aqueous phases was measured at different mass ratios and temperatures. It was observed that this parameter was mainly sensitive to the organic to aqueous mass ratio.

Two kinetic models were evaluated: hydrogen peroxide decomposition by  $\gamma$ -alumina and hydroxyl group oxidation at the surface. The heterogeneous liquid-liquid system assumed that the kinetics of mass transfer were faster than chemical reactions. In the first stage, kinetic models for the homogenous liquid system were developed, and then kinetics models for the liquid-liquid heterogeneous systems were developed. The calculation of the normalized posterior probability shows that the oxidation mechanism was the most probable model. A continuation of this work is to elucidate the reaction mechanism between hydrogen peroxide and hydroxyl group on alumina via density functional theory (DFT).

**Author Contributions:** Conceptualization, S.L.; methodology, D.D.M.D.B.; software, S.L.; validation, D.D.M.D.B.; formal analysis, D.D.M.D.B. and W.Y.P.-S.; investigation, D.D.M.D.B. and W.Y.P.-S.; writing—original draft preparation, S.L., D.D.M.D.B., T.S., and W.Y.P.-S.; writing—review and editing, V.C.M., S.L., D.D.M.D.B., T.S., and W.Y.P.-S.; supervision, S.L. and V.C.M. All authors have read and agreed to the published version of the manuscript.

**Funding:** The authors thank the ERASMUS program.

**Institutional Review Board Statement:** Not applicable.

**Informed Consent Statement:** Not applicable.

**Data Availability Statement:** Data available on request due to restrictions eg privacy or ethical.

**Conflicts of Interest:** The authors declare no conflict of interest.

## Appendix A

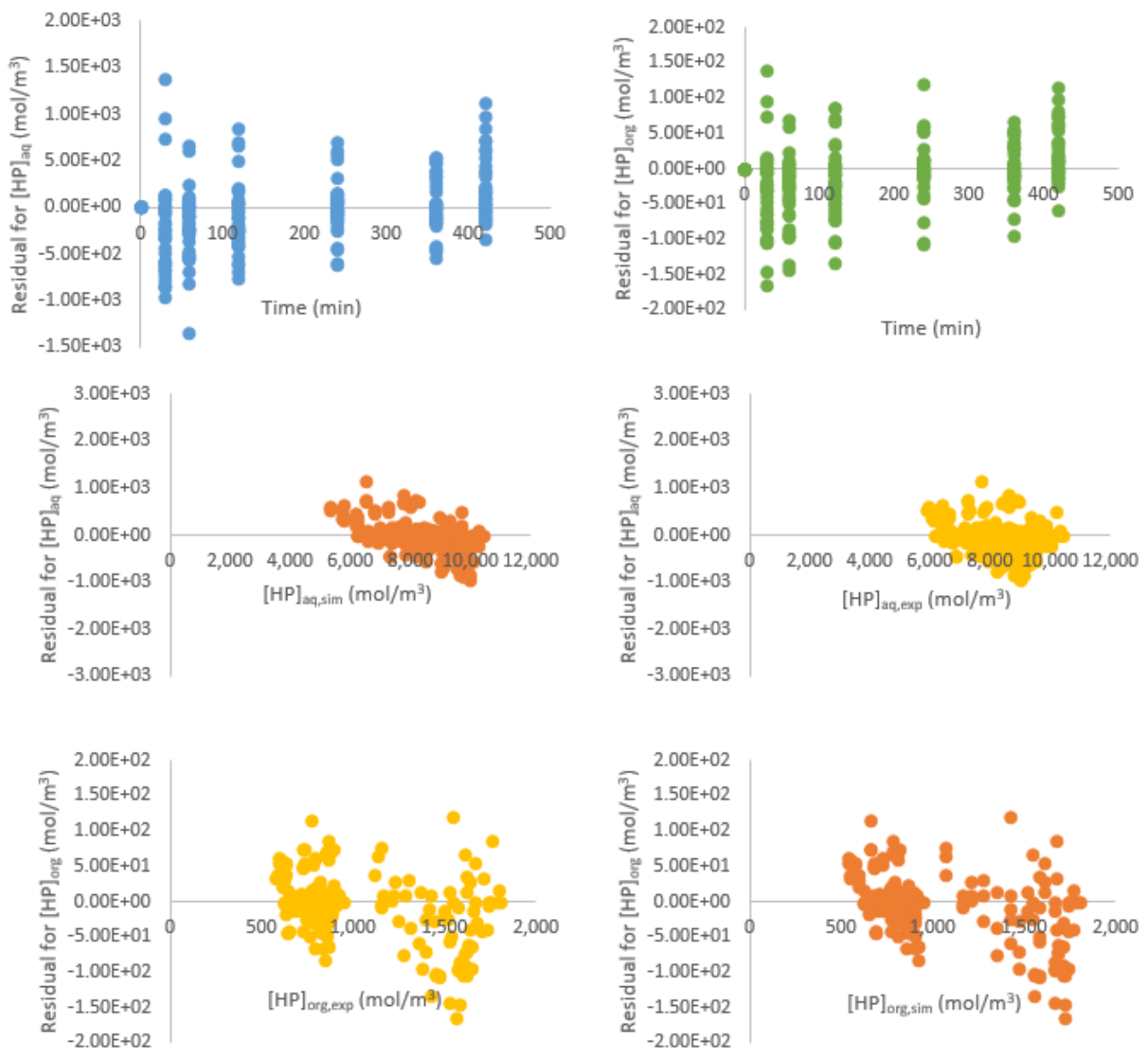


**Figure A1.** Distribution of residuals for Model d.

## Appendix B

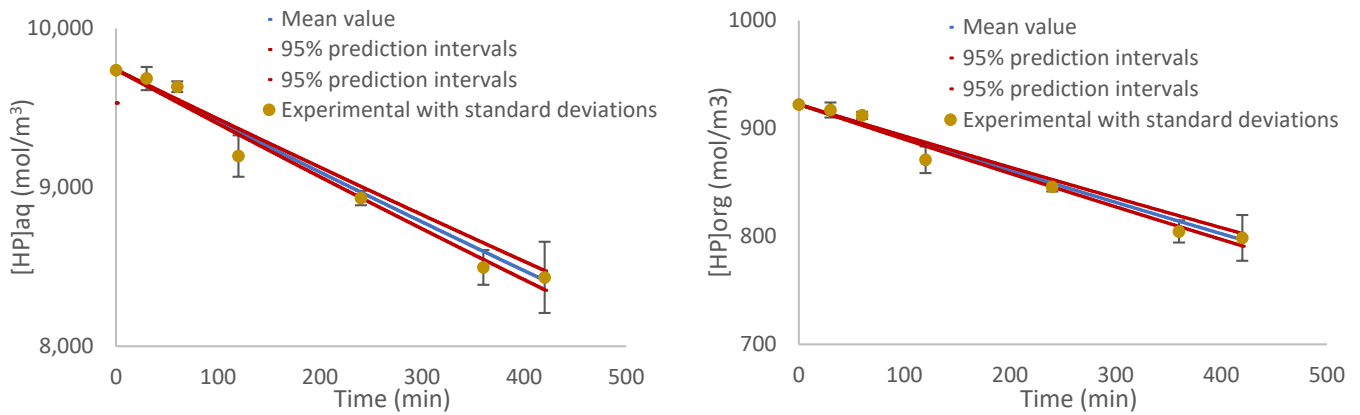


**Figure A2.** Prediction intervals of 95% for the concentration of hydrogen peroxide in the aqueous and organic phases, using the average of the experimental data and setting  $K_{1,org} = 0$  and  $K_{1,aq} = 15.05$  for Experiment 2.

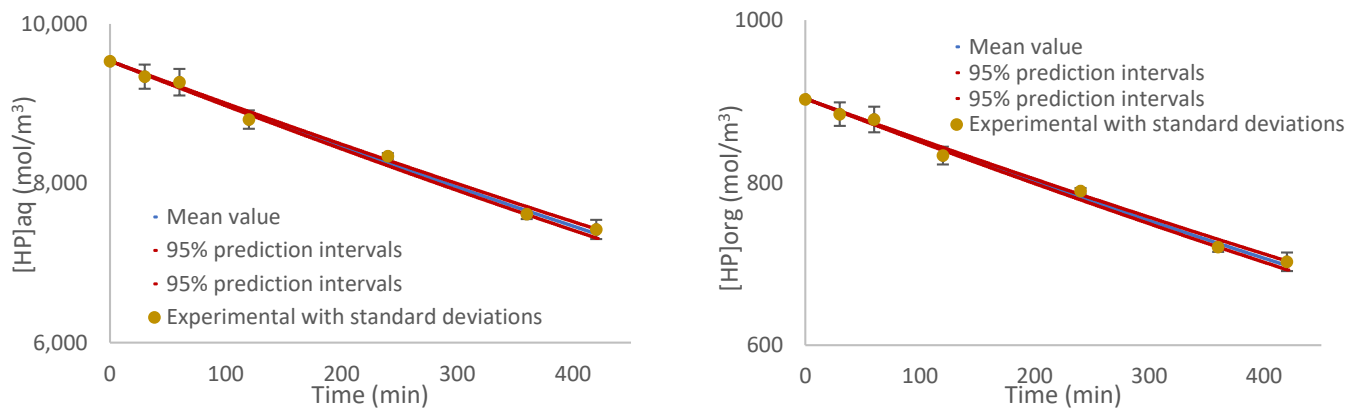


**Figure A3.** Prediction intervals of 95% for the concentration of hydrogen peroxide in the aqueous and organic phases, using the average of the experimental data and setting  $K_{1,org} = 0$  and  $K_{1,aq} = 15.05$  for Experiment 3.

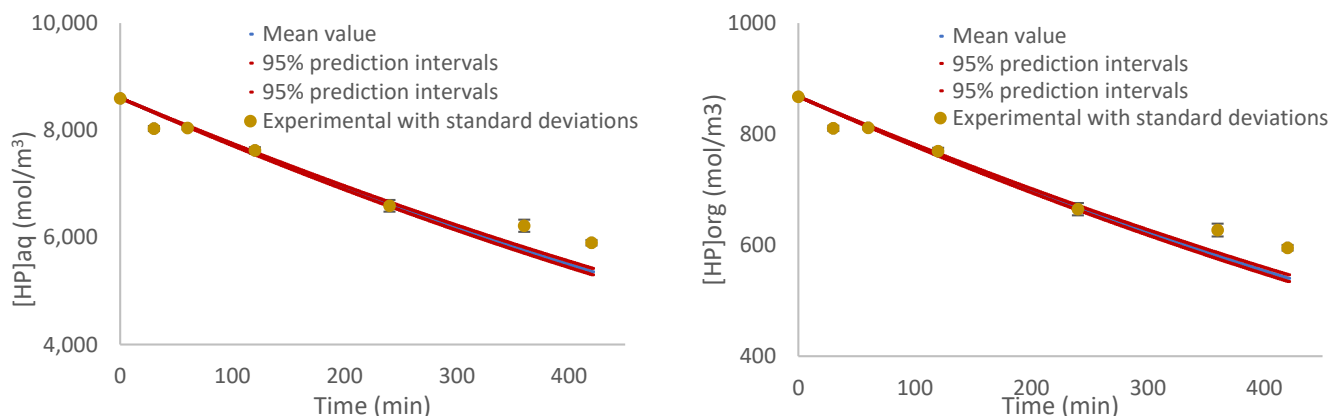


**Figure A4.** Prediction intervals of 95% for the concentration of hydrogen peroxide in the aqueous and organic phases, using the average of the experimental data and setting  $K_{1,org} = 0$  and  $K_{1,aq} = 15.05$  for Experiment 9.

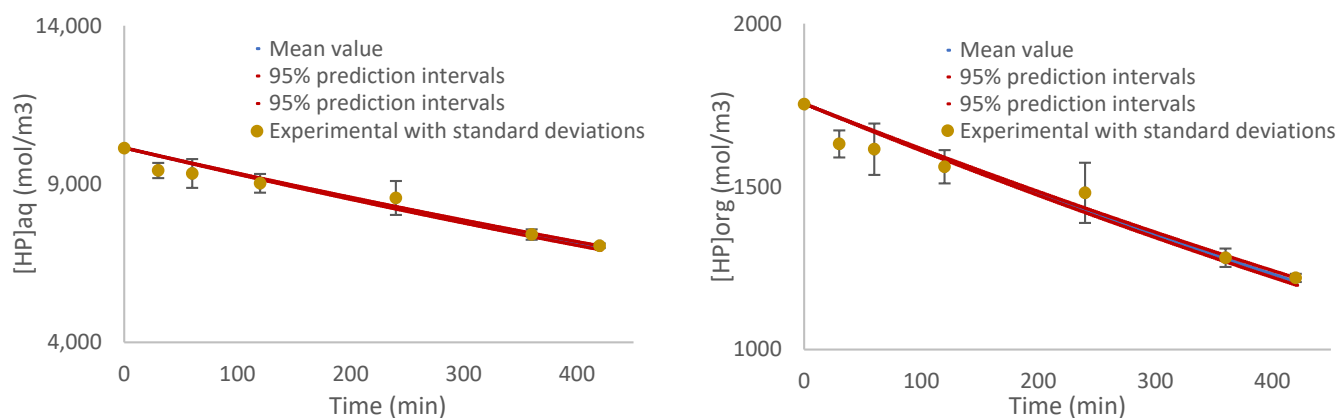


**Figure A5.** Prediction intervals of 95% for the concentration of hydrogen peroxide in the aqueous and organic phases, using the average of the experimental data and setting  $K_{1,org} = 0$  and  $K_{1,aq} = 15.05$  for Experiment 12.

## References

- Noyori, R.; Aoki, M.; Sato, K. Green oxidation with aqueous hydrogen peroxide. *Chem. Commun.* **2003**, *3*, 1977–1986. [[CrossRef](#)] [[PubMed](#)]
- Xie, H.L.; Fan, Y.X.; Zhou, C.H.; Du, Z.X.; Min, E.Z.; Ge, Z.H.; Li, X.N. A review on heterogeneous solid catalysts and related catalytic mechanisms for epoxidation of olefins with  $H_2O_2$ . *Chem. Biochem. Eng. Q.* **2008**, *22*, 25–39.
- Hauser, S.A.; Cokoja, M.; Kühn, F.E. Epoxidation of olefins with homogeneous catalysts-quo vadis? *Catal. Sci. Technol.* **2013**, *3*, 552–561. [[CrossRef](#)]
- Mandelli, D.; Van Vliet, M.C.A.; Sheldon, R.A.; Schuchardt, U. Alumina-catalyzed alkene epoxidation with hydrogen peroxide. *Appl. Catal. A Gen.* **2001**, *219*, 209–213. [[CrossRef](#)]
- Rinaldi, R.; Fujiwara, F.Y.; Schuchardt, U. Chemical and physical changes related to the deactivation of alumina used in catalytic epoxidation with hydrogen peroxide. *J. Catal.* **2007**, *245*, 456–465. [[CrossRef](#)]
- Uguina, M.A.; Delgado, J.A.; Rodríguez, A.; Carretero, J.; Gómez-Díaz, D. Alumina as heterogeneous catalyst for the regioselective epoxidation of terpenic diolefins with hydrogen peroxide. *J. Mol. Catal. A Chem.* **2006**, *256*, 208–215. [[CrossRef](#)]
- van Vliet, M.C.A.; Mandelli, D.; Arends, I.W.C.E.; Schuchardt, U.; Sheldon, R.A. Alumina: A cheap, active and selective catalyst for epoxidations with (aqueous) hydrogen peroxide. *Green Chem.* **2001**, *3*, 243–246. [[CrossRef](#)]
- Tian, Q.; Zhang, Z.; Zhou, F.; Chen, K.; Fu, J.; Lu, X.; Ouyang, P. Role of Solvent in Catalytic Conversion of Oleic Acid to Aviation Biofuels. *Energy Fuels* **2017**, *31*, 6163–6172. [[CrossRef](#)]
- Ding, Y.; Zhao, W.; Hua, H.; Ma, B.  $[\pi-C_5H_5N(CH_2)_{15}CH_3]_3[PW_4O_{32}]/H_2O_2$ /ethyl acetate/alkenes: A recyclable and environmentally benign alkenes epoxidation catalytic system. *Green Chem.* **2008**, *10*, 910–913. [[CrossRef](#)]
- Abdullah, B.M.; Salimon, J. Epoxidation of vegetable oils and fatty acids: Catalysts, methods and advantages. *J. Appl. Sci.* **2010**, *10*, 1545–1553. [[CrossRef](#)]
- Sepulveda, J.; Teixeira, S.; Schuchardt, U. Alumina-catalyzed epoxidation of unsaturated fatty esters with hydrogen peroxide. *Appl. Catal. A Gen.* **2007**, *318*, 213–217. [[CrossRef](#)]
- Kijewski, H.; Troe, J. Study of the pyrolysis of  $H_2O_2$  in the presence of  $H_2$  and CO by use of UV absorption of  $HO_2$ . *Int. J. Chem. Kinet.* **1971**, *3*, 223–235. [[CrossRef](#)]
- Perez-Sena, W.Y.; Wärnå, J.; Eränen, K.; Tolvanen, P.; Estel, L.; Leveneur, S.; Salmi, T. Use of semibatch reactor technology for the investigation of reaction mechanism and kinetics: Heterogeneously catalyzed epoxidation of fatty acid esters. *Chem. Eng. Sci.* **2021**, *230*, 116206. [[CrossRef](#)] [[PubMed](#)]
- Murzin, D.Y.; Wärnå, J.; Haario, H.; Salmi, T. Parameter estimation in kinetic models of complex heterogeneous catalytic reactions using Bayesian statistics. *React. Kinet. Mech. Catal.* **2021**, *133*, 1–15. [[CrossRef](#)]
- Casson Moreno, V.; Battaglia, E.; Maschio, G. Hydrogen peroxide decomposition analysis by screening calorimetry technique. *Chem. Eng. Trans.* **2012**, *26*, 27–32. [[CrossRef](#)]
- Klöker, M.; Kenig, E.Y.; Górak, A.; Markusse, A.P.; Kwant, G.; Moritz, P. Investigation of different column configurations for the ethyl acetate synthesis via reactive distillation. *Chem. Eng. Process. Process Intensif.* **2004**, *43*, 791–801. [[CrossRef](#)]
- Zheng, J.L.; Wärnå, J.; Salmi, T.; Burel, F.; Taouk, B.; Leveneur, S. Kinetic modeling strategy for an exothermic multiphase reactor system: Application to vegetable oils epoxidation using Prileschajew method. *AIChE J.* **2016**, *62*, 726–741. [[CrossRef](#)]
- Stewart, W.E.; Caracotsios, M. *Computer-Aided Modeling of Reactive Systems*; Wiley & Sons: Hoboken, NJ, USA, 2008; ISBN 9780470274958.
- Stewart, W.E.; Caracotsios, M. Athena Visual Studio. Available online: [www.athenavisual.com](http://www.athenavisual.com) (accessed on 10 June 2020).